Nanoscale Advances

COMMUNICATION

View Article Online
View Journal | View Issue

Cite this: *Nanoscale Adv.*, 2019, **1**, 508

Optically active quantum dots with induced circularly polarized luminescence in amphiphilic peptide dendron hydrogel†

Chengxi Li,[abc] Xue Jin,[a] Tonghan Zhao,[ab] Jin Zhou[a] and Pengfei Duan *[ab]

Received 17th September 2018
Accepted 25th October 2018

DOI: 10.1039/c8na00216a

rsc.li/nanoscale-advances

In this study, water-soluble semiconductor quantum dots (QDs) showing induced circularly polarized luminescence (CPL) in an organic–inorganic coassembled hydrogel were demonstrated. Achiral QDs could be encapsulated into a chiral peptide dendron hydrogel through cogelation. These cogels displayed intense induced circularly polarized emission. In addition, the direction of the CPL property of QD cogels could be regulated by the supramolecular chirality of hydrogels. Our findings reveal that the emergence of CPL achiral QDs can be triggered by the chirality transfer in a multiple-component dendron hydrogel system. This study has given a new understanding into the design of functional chiroptical materials.

Chiroptical materials showing circularly polarized luminescence (CPL) have been attracting increasing attention due to their great potentials in various research fields from optical science to biology.[1–5] The development of novel and highly efficient CPL-active materials is an urgent issue in chiral science. For achieving CPL-active materials, great interest has been generated in the construction of chiral and emissive center structures.[6–8] Generally, the following two approaches for fabricating CPL-active materials are commonly used. One is introducing a chiral center to emitters, including organic molecules,[8–12] metal–organic complexes,[13] crystals,[14,15] and nano-/micro-structures,[16–21] which involves tedious synthesis. Another pathway can be called the "guest–host" mode. Achiral emitters can be encapsulated into a chiral matrix, which can display induced CPL. The latter approach is more convenient for the design of CPL-active materials with tunable CPL intensities and wavelengths since luminescent species and chiral hosts can have a variety of combinations. To date, most of the reported CPL-active inorganic materials[22,23] have been fabricated through this approach.

Although the method to obtain CPL-active materials is no longer one of the novel issues, most of the materials are obtained from the organic phase, which goes against the principles of cost reduction and green chemistry.[22–25] Hence, developing biocompatible CPL-active materials in an aqueous phase is necessary for practical applications[26–32] and further understanding of chiral optics in biological systems.[4,5,33,34] Herein, we report a general method to achieve CPL-active hydrogels with various emission wavelengths simply by blending achiral chalcogenide semiconductor quantum dots (QDs) with an amphiphilic peptide dendron. It has been reported that CPL-active QDs can be obtained by modifying achiral QDs with chiral capping reagents.[35,36] However, to date, only chiral cysteine has been used as the capping reagent because of strong conjugating ability of the thiol group. The only example of CPL-active QDs fabricated without cysteine was achieved by loading quantum dots with a chiral cavity of a protein nanocage. It was argued that the QDs in this protein nanocage exhibited a chiral crystal arrangement that led to CPL activity.[37] Although this approach is useful, the synthesis or selection of an appropriate chiral host matrix involves an immense amount of time and effort. It is desired to develop a more straightforward approach for obtaining CPL-active QDs with various colours and sizes in aqueous solutions *via* a simple blending method. In this study, we show a simple and versatile methodology to achieve stable circularly polarized emission in supramolecular hydrogel *via* QD-peptide dendron co-assembly.

As a proof of concept, we improved the gelatinization ability in water by extending the length of alkyl chain of a well-demonstrated peptide dendron hydrogelator.[38] The new hydrogelator *N*-behenic-1,5-bis(L/D-glutamic acid)-L/D-glutamic diamide (L-/D-BGAc), as shown in Fig. 1a, exhibited excellent hydrogelation behaviour with a low critical gelation

[a]*CAS Key Laboratory of Nanosystem and Hierarchical Fabrication, CAS Center for Excellence in Nanoscience, Division of Nanophotonics, National Center for Nanoscience and Technology (NCNST), No. 11 ZhongGuanCun BeiYiTiao, Beijing 100190, P. R. China. E-mail: duanpf@nanoctr.cn; Tel: +86-10-82545510*

[b]*School of Nanoscience and Technology, University of Chinese Academy of Sciences, Beijing 100049, P. R. China*

[c]*College of Chemistry, Key Lab of Environment-Friendly Chemistry and Application of the Ministry of Education, Xiangtan University, Xiangtan 411105, P. R. China*

† Electronic supplementary information (ESI) available. See DOI: 10.1039/c8na00216a

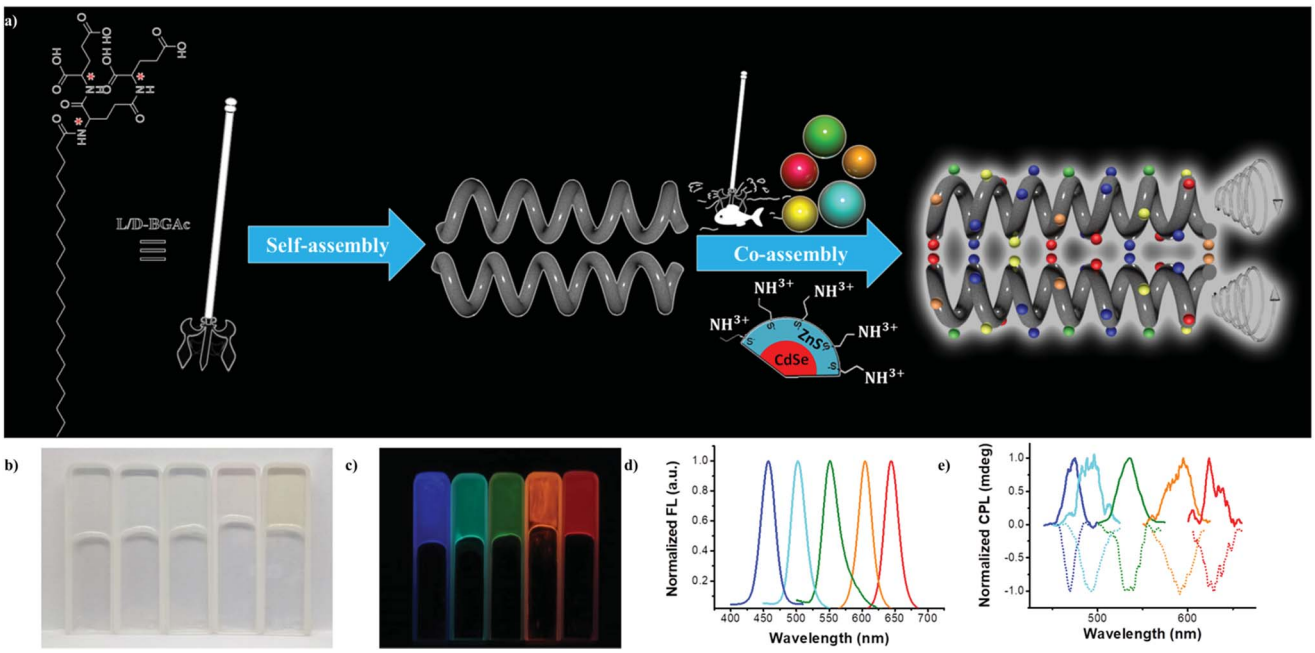

Fig. 1 (a) Molecular structure of the gelators and the construction of the used QDs; a schematic diagram about QDs-hydrogel showing CPL activity under UV 365 nm irradiation. The QDs with CdSe core and ZnS shell capped with 2-aminoethanethiol hydrochloride are used in this work. (b) The morphology of the corresponding cogel upon white light irradiation. (c) The photo of the cogel upon 365 nm UV light. (d) Fluorescence spectra of the QDs/BGAc cogels; $\lambda_{ex} = 360$ nm. (e) Symmetric CPL spectra of the QDs/BGAc cogels; $\lambda_{ex} = 360$ nm. [BGAc] = 6 mg mL^{-1}; [QDs] = 0.2 mg mL^{-1}.

concentration (CGC). Various achiral QDs capped with 2-aminoethanethiol could be captured by the multiple carboxyl groups in L-/D-BGAc, as illustrated by harpoon fishing (Fig. 1a). The co-assembled hydrogels showed strong photoluminescence and intense circularly polarized emission.

Here, a convergent method (Fig. S1, ESI†) was employed to synthesize two enantiopure hydrogelators (L-BGAc and D-BGAc) used in this study. BGAc can form a transparent hydrogel immediately after a heating-cooling treatment. For cogel fabrication, experimentally, an aqueous solution of QDs was added into an aqueous dispersion of BGAc. The mixture was heated to 90 °C until the solids were completely dissolved. After cooling to room temperature, it could stand for one hour to obtain a hydrogel doped with different QDs (Fig. 1b). Under UV 365 nm irradiation, the obtained hydrogel exhibited bright luminescence in five colors from blue to red (Fig. 1c), and the corresponding luminescence spectra are shown in Fig. 1d. The luminescence spectra of the hydrogels showed an identical shape compared with the one obtained from QD aqueous solution (Fig. S2, ESI†), which indicated that the emissive properties of QDs in cogels were well preserved.

Notably, all the obtained hydrogels with various emissive QDs showed strong CPL emission. Some special features are given below for the CPL properties in this QD-doped gel. Intense mirror-image CPL spectra could be generated for the cogels, which were regulated by the chirality of hydrogelators. A positive CPL signal was observed in QDs/D-BGAc samples, whereas a negative signal was obtained in cogels of QDs/L-BGAc samples. For instance, strong mirror-image CPL (Fig. S4, ESI†) was exhibited by the cyan QDs in the cogel, corresponding to the gelator of opposite molecular chirality. As shown in Fig. 1e, CPL spectra of various cogels exhibited signals with different handedness from 400 to 750 nm, enabling circularly polarized emission covering the full range of visible light.

The magnitude of CPL can be evaluated by the luminescence dissymmetry factor (g_{lum}), which is defined as $g_{lum} = 2 \times (I_L - I_R)/(I_L + I_R)$, where I_L and I_R refer to the intensities of left-handed and right-handed circularly polarized light, respectively.[39] Experimentally, CPL was measured using a JASCO CPL-200 spectrometer, and the value of g_{lum} was obtained as $g_{lum} = 2 \times$ [ellipticity/(32 980/ln10)]/total fluorescence intensity at the CPL extremum. The calculated value of the dissymmetry factor $|g_{lum}|$ of the CPL signal was from 10^{-2} to 10^{-3} (Table S1, ESI†), whereas a maximum value was observed in the green QD sample under 360 nm laser (3.26×10^{-2}), which is a remarkable value than that observed for other inorganic nanomaterials such as cysteine-capped CdSe nanoparticles.[35] In addition, supramolecular assembly was obtained through simple blending without tedious inorganic synthesis.

To investigate the microstructures, atomic force microscopy (AFM) and transmission electron microscopy (TEM) were used to examine the dried xerogel. Fig. 2 exhibits the nanostructures from BGAc hydrogel and cogel of BGAc with QDs. As shown in Fig. 2a and b, BGAc was found to form fibrous structures in water with long fiber structures. To further check the characteristics of these fibrous microstructures, TEM was applied. As shown in Fig. 2c and d, TEM negative stain images confirmed that the 1D structure of assemblies was typically a solid fibrous

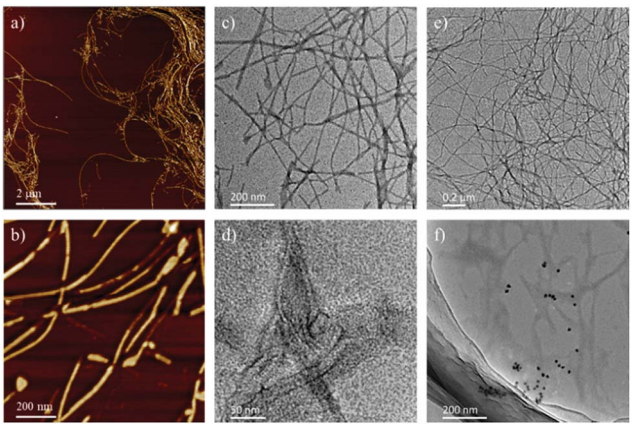

Fig. 2 (a and b) AFM analysis of nanofibers formed by BGAc in hydrogel on different scale and (c and d) those negatively stained *via* uranyl acetate under TEM. (e and f) Morphology of QDs/BGAc co-assemblies by TEM analysis.

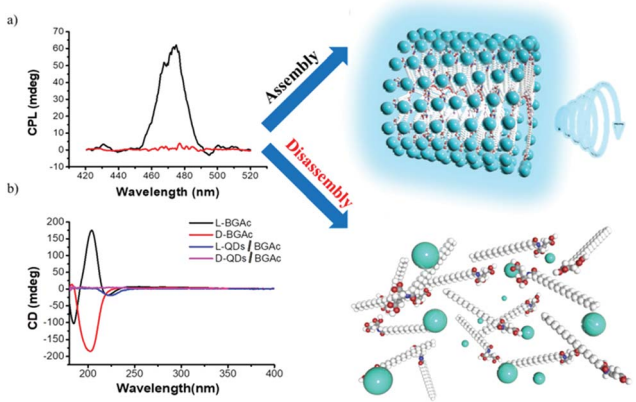

Fig. 3 (a) CPL spectra of cyan-emissive QD-doped co-gels in the state of assembly (black line) and disassembly (red line). The spectrum of disassembly state was obtained with solution by heating, in which no CPL occurred, but after cooling to rt., hydrogel was obtained and CPL signal appeared. λ_{ex} = 360 nm. [BGAc] = 6 mg mL^{-1}; [QDs] = 0.2 mg mL^{-1}. (b) The contrast CD spectrum diagram of pre and post introducing QDs. ([QDs] = 0.2 mg mL^{-1}, [L-/D-BGAc] = 6 mg mL^{-1}).

structure. This is completely different from the observations for the analogue hydrogelator that has a relatively short alkyl chain. Very thin nanotube structures could be observed in the hydrogel formed by short chain gelators.[38] Slight changes in the molecular structure resulted in completely different assembled structures (Fig. S5, ESI†). In this study, after blending with QDs, a similar nanofiber structure was retained. It should be noted that since rare QDs and nanotubes do not exhibit a pure homogeneous system, some slight aggregation of QDs can be found in this sample. However, the assembled QDs obtain the chirality from the chiral nanofiber. Hence, based on previous studies,[23,35,36] there were two conjectures of the induced CPL in the cogels. First, one reason for the chirality of QDs is the chiral arrangement of QDs induced by self-assembled chiral networks. Second, the assembled peptide dendron can endow chirality to the QDs through ligand-exchange with mercaptoethylamine on the surface of the QDs in water.

To verify the above two conjectures, the CPL properties of the disassembled state of the QDs/gelator complex were tested. Upon heating to about 90 °C, the compound of 0.2 mg mL^{-1} QDs and 6 mg mL^{-1} BGAc could be dissolved in water. Using 360 nm excitation, the mixture solution exhibited strong emission, but no CPL signal was observed (Fig. 3a). The obtained cogel was a thermo-responsive gel, which could be heated to solution state again around 50 °C. The amount of doped QDs was kept at 0.2 mg mL^{-1}, which is a maximum value. The cogel could be destroyed if excess QDs were added to the cogel. The gel–sol transition temperature of the cogel was almost the same as that of pure hydrogel. There was no clear effect of such a process on the size of QDs. The result seems to be consistent with the above hypothesis. This can be further confirmed by circular dichroism (CD) testing. After addition of QDs to the hydrogel, it is expected that the CD signal of QDs can confirm chiral arrangement of QDs. However, due to weak absorption (Fig. S3, ESI†), no CD signal of QDs was obtained, as verified by the mirror-image CD spectra in Fig. 3b. Fortunately, it was observed that the intensity of CD signal around 212 nm, for the absorption band of hydrogel, decreased after QDs were added. These changes clearly indicated that the β-sheet conformation of assembly in the part of the amide group was destroyed[38,40–42] because of the interaction between carboxyl groups and ligands of QDs.

The interaction between QDs and gelator could be further examined *via* X-ray diffraction (XRD) and Fourier transform infrared (FTIR) spectroscopy, as illustrated in Fig. 4a and b, respectively. According to XRD analysis, the nanofiber showed a strong single diffraction peak at 2.143°, which corresponded to the distance of 41.19 Å. By considering the molecular structure using space-filling models (CPK model), the molecular length of BGAc was estimated to be 32 Å. The *d*-spacing value

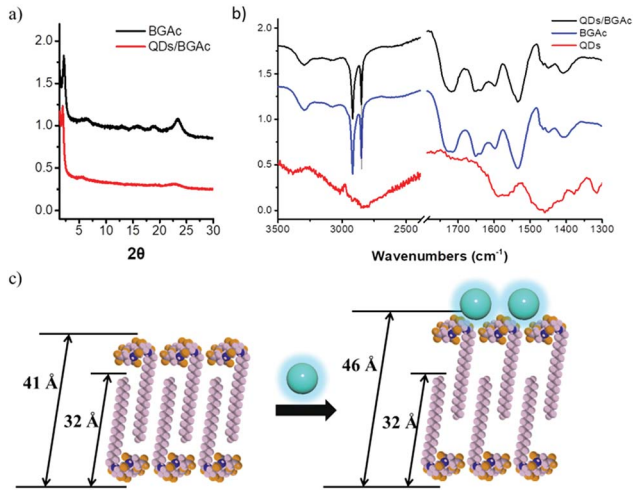

Fig. 4 (a) XRD analysis of hydrogel made from BGAc and the QD-doped cogel. (b) FTIR analysis of co-assemblies and each component. (c) Schematic diagram of the influence of QDs on arrangement of assemblies.

was between one and two layers of molecular thickness, which indicated that the peptide dendron molecules formed a partially overlapping bilayer structure.[38] More interestingly, after forming the cogel, a strong single diffraction peak at 1.909 was observed in the XRD pattern in the small-angle region, corresponding to a *d*-spacing value of 46.24 Å; this suggested that the BGAc molecules wrapped around QDs resulted in the reduction of the hydrogen bonds in the fibrous assemblies, which in turn could expand the layer spacing of the bilayer, as shown in Fig. 4c. The XRD pattern indicated that after forming the cogel with QDs, the well-ordered structure was almost the same as that of pure hydrogel. The existence of molecular interactions between the QDs and the gelator was investigated by FTIR analysis. For BGAc and QDs/BGAc xerogels, the occurrence of $\nu_{C=O}$ bands at 1724 cm^{-1} and 1711 cm^{-1}, respectively, indicated that the interaction formed by the –COOH groups contains both lateral inter- and intra-molecular H-bonds, which is confirmed by the peak at 3072 cm^{-1}.[43] Meanwhile, the xerogels from BGAc with an aqueous solution of QDs were also studied. Two vibrational bands at 1724 cm^{-1} and 1711 cm^{-1} disappeared simultaneously, whereas the remaining one band was maintained at 1718 cm^{-1}. This indicated that the carboxylic acid groups of BGAc that had previously been involved in different kinds of H-bonds owing to stronger carboxylic acid–base interactions[44] now interacted exclusively with QDs capped with aminoethanethiol. The vibration bands at 2917 cm^{-1} and 2850 cm^{-1} confirmed CH_2 antisymmetrical and symmetrical stretching vibrations, respectively, suggesting highly ordered conformation of alkyl chains.[44–46] The amide I and amide II bands at 1654 cm^{-1} and 1535 cm^{-1} revealed that many hydrogen bonds were still formed between amide groups; thus, efficient preservation of the nanofiber structure was explained. However, due to the –C═O group with one hydrogen bond ligand molecule, it demonstrated a new strong vibrational band at around 1545 cm^{-1} upon mixing,[43,47] which agreed with the formation of atypical β-sheets (Fig. S6, ESI†). Thus, since hydrogen bonding and electrostatic interactions between aminoethanethiol-capped CdSe/ZnS QDs and the carboxylic groups of the gelator played significant roles, the co-assembly behaviour of the CPL-active hydrogel obtained by chiral arrangement of QDs could be further considered.

Conclusions

CPL-active hydrogels were successfully prepared by supramolecular self-assembly of achiral QDs and chiral peptide dendron gelators. Various achiral QDs were encapsulated into the peptide dendron hydrogels during the process of co-assembly, enabling the emission of induced CPL with a large range of wavelength from blue to red. The chiral arrangement of doped QDs played a significant role for the induced CPL. The direction of induced CPL signal can be tailored by the chirality of peptide dendron. To develop biocompatible CPL-active materials, supramolecular cogelation of achiral inorganic emissive nanomaterials and a chiral gelator can afford a novel idea for obtaining potential applications for functional chiroptical materials.

Conflicts of interest

There are no conflicts to declare.

Acknowledgements

This work was supported by Ministry of Science and Technology of the People's Republic of China (2016YFA0203400, 2017YFA0206600), National Natural Science Foundation of China (51673050, 21802027), P. D. thanks for the supporting of "New Hundred-Talent Program" research fund from the Chinese Academy of Sciences.

Notes and references

1 J. Yeom, B. Yeom, H. Chan, K. W. Smith, S. Dominguez-Medina, J. H. Bahng, G. P. Zhao, W. S. Chang, S. J. Chang, A. Chuvilin, D. Melnikau, A. L. Rogach, P. J. Zhang, S. Link, P. Kral and N. A. Kotov, *Nat. Mater.*, 2015, **14**, 66–72.
2 P. Y. Xing and Y. L. Zhao, *Acc. Chem. Res.*, 2018, **51**, 2324–2334.
3 Y. Zhao, N. A. A. Rahirn, Y. J. Xia, M. Fujiki, B. Song, Z. B. Zhang, W. Zhang and X. L. Zhu, *Macromolecules*, 2016, **49**, 3214–3221.
4 R. M. Templin, M. J. How, N. W. Roberts, T. H. Chiou and J. Marshall, *J. Exp. Biol.*, 2017, **220**, 3222–3230.
5 W. A. Bonner and E. Rubenstein, *Biosystems*, 1987, **20**, 99–111.
6 Y. Yang, R. C. da Costa, D. M. Smilgies, A. J. Campbell and M. J. Fuchter, *Adv. Mater.*, 2013, **25**, 2624–2628.
7 S. C. J. Meskers, E. Peeters, B. M. W. Langeveld-Voss and R. A. J. Janssen, *Adv. Mater.*, 2000, **12**, 589–594.
8 R. Tempelaar, A. Stradomska, J. Knoester and F. C. Spano, *J. Phys. Chem. B*, 2011, **115**, 10592–10603.
9 J. Z. Liu, H. M. Su, L. M. Meng, Y. H. Zhao, C. M. Deng, J. C. Y. Ng, P. Lu, M. Faisal, J. W. Y. Lam, X. H. Huang, H. K. Wu, K. S. Wong and B. Z. Tang, *Chem. Sci.*, 2012, **3**, 2737–2747.
10 Z. C. Shen, T. Y. Wang, L. Shi, Z. Y. Tang and M. H. Liu, *Chem. Sci.*, 2015, **6**, 4267–4272.
11 J. Kumar, T. Nakashima and T. Kawai, *Langmuir*, 2014, **30**, 6030–6037.
12 J. Kumar, H. Tsumatori, J. Yuasa, T. Kawai and T. Nakashima, *Angew. Chem., Int. Ed.*, 2015, **54**, 5943–5947.
13 R. Carr, N. H. Evans and D. Parker, *Chem. Soc. Rev.*, 2012, **41**, 7673–7686.
14 B. A. San Jose, J. L. Yan and K. Akagi, *Angew. Chem., Int. Ed.*, 2014, **53**, 10641–10644.
15 J. R. A. Moreno, J. J. L. Gonzalez, F. P. Urena, F. Vera, M. B. Ros and T. Sierra, *J. Phys. Chem. B*, 2012, **116**, 5090–5096.
16 S. S. Babu, V. K. Praveen and A. Ajayaghosh, *Chem. Rev.*, 2014, **114**, 1973–2129.

17 K. Ariga, J. B. Li, J. B. Fei, Q. M. Ji and J. P. Hill, *Adv. Mater.*, 2016, **28**, 1251–1286.
18 S. Yagai, S. Okamura, Y. Nakano, M. Yamauchi, K. Kishikawa, T. Karatsu, A. Kitamura, A. Ueno, D. Kuzuhara, H. Yamada, T. Seki and H. Ito, *Nat. Commun.*, 2014, **5**, 10.
19 T. Shimizu, M. Masuda and H. Minamikawa, *Chem. Rev.*, 2005, **105**, 1401–1443.
20 Y. Yamamoto, T. Fukushima, Y. Suna, N. Ishii, A. Saeki, S. Seki, S. Tagawa, M. Taniguchi, T. Kawai and T. Aida, *Science*, 2006, **314**, 1761–1764.
21 Y. Y. Duan, X. Liu, L. Han, S. Asahina, D. D. Xu, Y. Y. Cao, Y. Yao and S. N. Che, *J. Am. Chem. Soc.*, 2014, **136**, 7193–7196.
22 Y. H. Shi, P. F. Duan, S. W. Huo, Y. G. Li and M. H. Liu, *Adv. Mater.*, 2018, **30**, 1705011.
23 S. W. Huo, P. F. Duan, T. F. Jiao, Q. M. Peng and M. H. Liu, *Angew. Chem., Int. Ed.*, 2017, **56**, 12174–12178.
24 Y. Nakano and M. Fujiki, *Macromolecules*, 2011, **44**, 7511–7519.
25 T. Goto, Y. Okazaki, M. Ueki, Y. Kuwahara, M. Takafuji, R. Oda and H. Ihara, *Angew. Chem., Int. Ed.*, 2017, **56**, 2989–2993.
26 M. Grell, M. Oda, K. S. Whitehead, A. Asimakis, D. Neher and D. D. C. Bradley, *Adv. Mater.*, 2001, **13**, 577.
27 E. Peeters, M. P. T. Christiaans, R. A. J. Janssen, H. F. M. Schoo, H. Dekkers and E. W. Meijer, *J. Am. Chem. Soc.*, 1997, **119**, 9909–9910.
28 Y. H. Geng, A. Trajkovska, S. W. Culligan, J. J. Ou, H. M. P. Chen, D. Katsis and S. H. Chen, *J. Am. Chem. Soc.*, 2003, **125**, 14032–14038.
29 C. Wagenknecht, C. M. Li, A. Reingruber, X. H. Bao, A. Goebel, Y. A. Chen, Q. A. Zhang, K. Chen and J. W. Pan, *Nat. Photonics*, 2010, **4**, 549–552.
30 Y. Yang, R. C. da Costa, M. J. Fuchter and A. J. Campbell, *Nat. Photonics*, 2013, **7**, 634–638.
31 Y. Kim, B. Yeom, O. Arteaga, S. J. Yoo, S. G. Lee, J. G. Kim and N. A. Kotov, *Nat. Mater.*, 2016, **15**, 461.
32 H. Z. Chen and Y. L. Zhao, *ACS Appl. Mater. Interfaces*, 2018, **10**, 21021–21034.
33 H. Wynberg, E. W. Meijer, J. C. Hummelen, H. Dekkers, P. H. Schippers and A. D. Carlson, *Nature*, 1980, **286**, 641–642.
34 T. G. Bromage, H. M. Goldman, S. C. McFarlin, J. Warshaw, A. Boyde and C. M. Riggs, *Anat. Rec., Part B*, 2003, **274**, 157–168.
35 U. Tohgha, K. K. Deol, A. G. Porter, S. G. Bartko, J. K. Choi, B. M. Leonard, K. Varga, J. Kubelka, G. Muller and M. Balaz, *ACS Nano*, 2013, **7**, 11094–11102.
36 J. J. Cheng, J. J. Hao, H. C. Liu, J. G. Li, J. Z. Li, X. Zhu, X. D. Lin, K. Wang and T. C. He, *ACS Nano*, 2018, **12**, 5341–5350.
37 M. Naito, K. Iwahori, A. Miura, M. Yamane and I. Yamashita, *Angew. Chem., Int. Ed.*, 2010, **49**, 7006–7009.
38 P. Duan, L. Qin, X. Zhu and M. Liu, *Chem.–Eur. J.*, 2011, **17**, 6389–6395.
39 N. Berova, K. Nakanishi, R. W. Woody and R. Woody, *Circular dichroism: principles and applications*, John Wiley & Sons, 2000.
40 J. E. Goldberger, E. J. Berns, R. Bitton, C. J. Newcomb and S. I. Stupp, *Angew. Chem., Int. Ed.*, 2011, **50**, 6292–6295.
41 L. Qin, P. Duan, F. Xie, L. Zhang and M. Liu, *Chem. Commun.*, 2013, **49**, 10823–10825.
42 S. R. Bull, M. O. Guler, R. E. Bras, T. J. Meade and S. I. Stupp, *Nano Lett.*, 2005, **5**, 1–4.
43 P. Gao, C. L. Zhan, L. Z. Liu, Y. B. Zhou and M. H. Liu, *Chem. Commun.*, 2004, 1174–1175.
44 X. F. Zhu, P. F. Duan, L. Zhang and M. H. Liu, *Chem.–Eur. J.*, 2011, **17**, 3429–3437.
45 C. L. Zhan, P. Gao and M. H. Liu, *Chem. Commun.*, 2005, 462–464.
46 P. Gao, C. L. Zhan and M. H. Liu, *Langmuir*, 2006, **22**, 775–779.
47 J. Y. Lee, P. C. Painter and M. M. Coleman, *Macromolecules*, 1988, **21**, 954–960.